

Figure S1. Spearman correlations between neutralization profiles of C117 and C110 plasma isolates and neutralization profiles of bNAbs HEPC3, HEPC74, HEPC43, and CBH-2, related to Figure 1. Neutralization profiles were defined using a panel of nineteen genotype 1 HCVpp. Each point indicates neutralization of a single HCVpp strain by the indicated mAb on the x-axis, and the indicated plasma sample on the y-axis. Spearman correlations (r) and two-sided p values are indicated for each comparison. (A) C117 plasma with autologous bNAb HEPC3. (B) C110 plasma with autologous bNAbs HEPC74 (top) and HEPC43 (bottom). (C) C117 and C110 plasma correlation with negative control bNAb CBH-2.

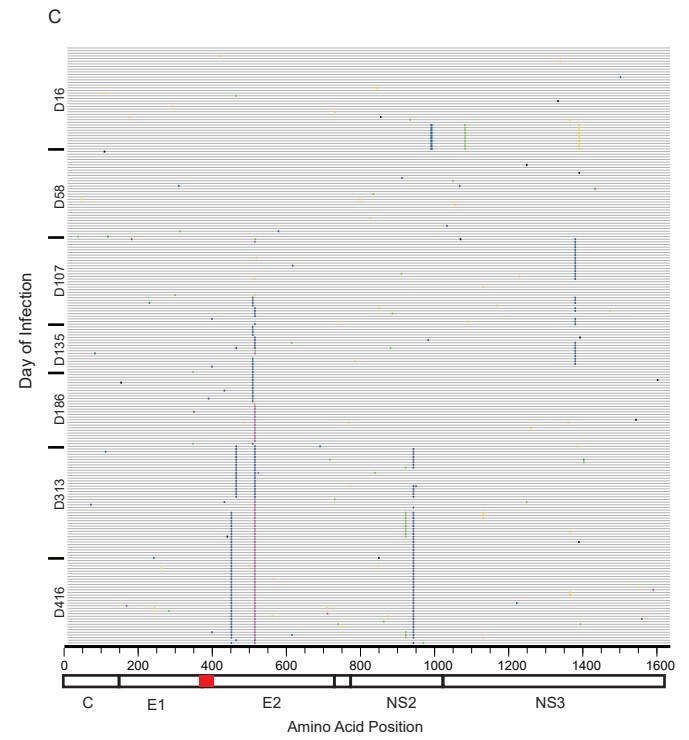
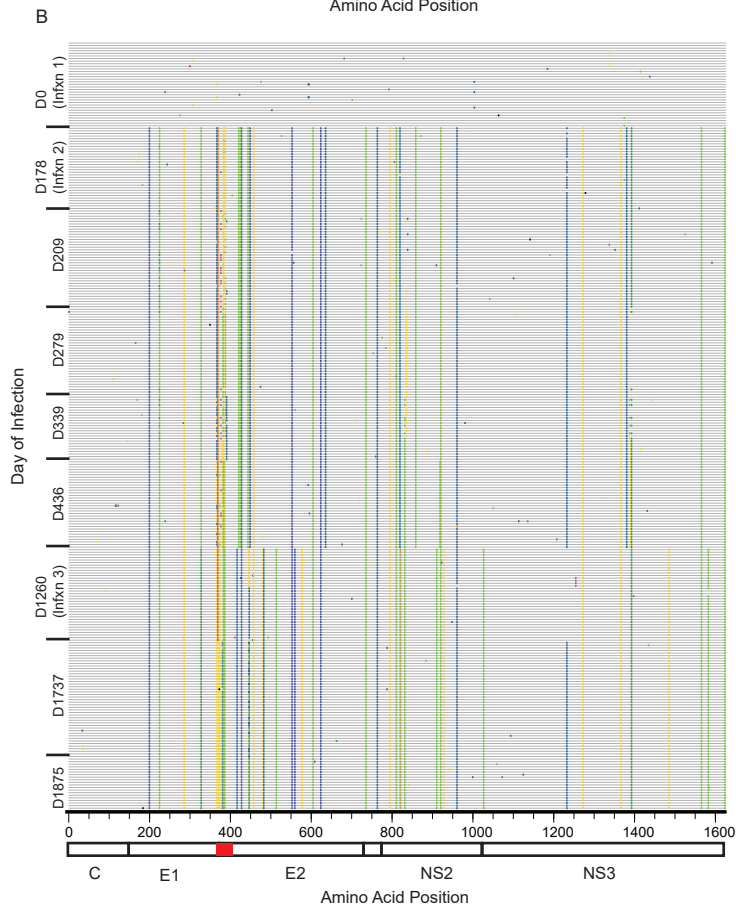
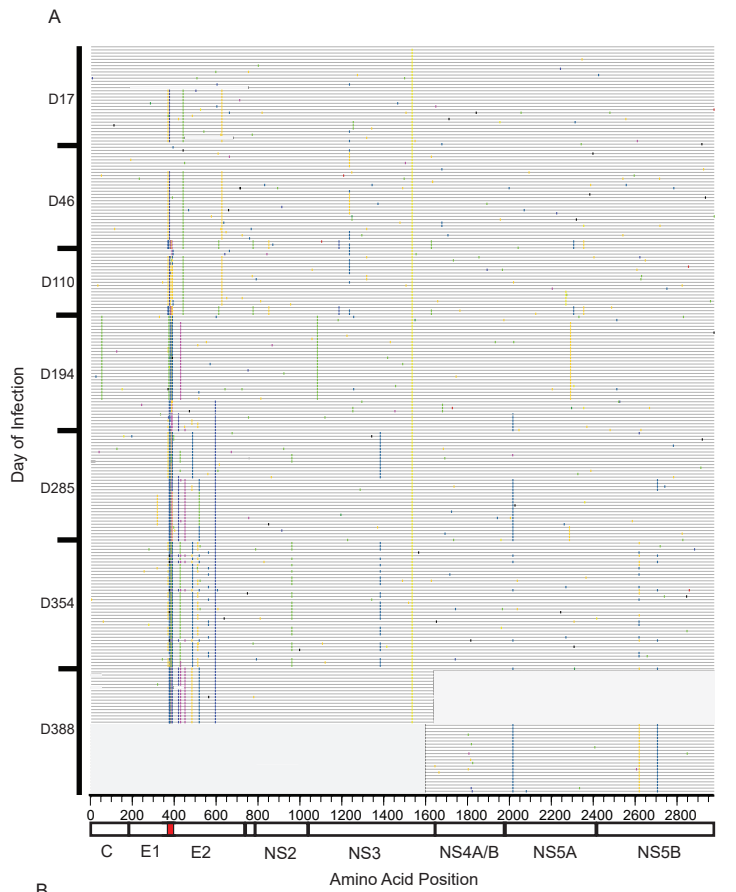


Figure S2. Highlighter plots indicating positions of amino acid differences in longitudinal viral sequences obtained by single-genome amplification from plasma of three subjects at time points throughout the course of infection, related to Figure 2. Amino acid differences from a master sequence are indicated by colored bars. Sequences are arranged by their date of isolation. Proteins are indicated, and hypervariable region 1 (HVR1) is highlighted in red. Numbering is relative to strain H77 polyprotein. **(A)** Full genome analysis of C117 infection. Amino acid changes relative to D17-1a53 (T/F#3) are identified. The sequence of the final circulating viral strain present immediately prior to clearance of infection was amplified in separate 5' and 3' hemigenomic reactions. **(B)** 5' hemigenomic analysis of C110 infection. Amino acid changes relative to both D0-A4 (Infxn 1) and Bole1a are identified. **(C)** 5' hemigenomic analysis of P29 infection. Amino acid changes relative to D16-B11 (T/F#1) are identified.

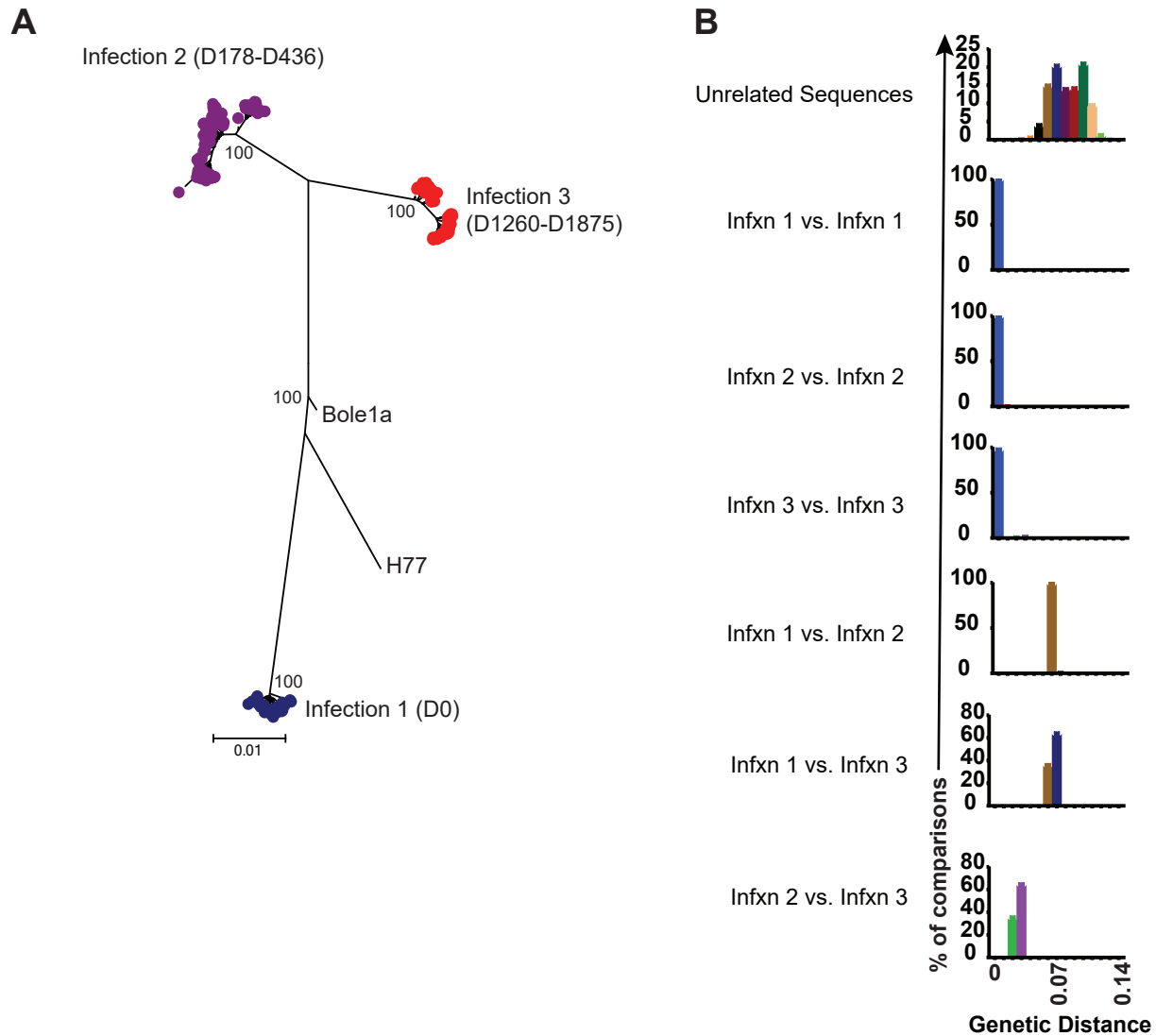
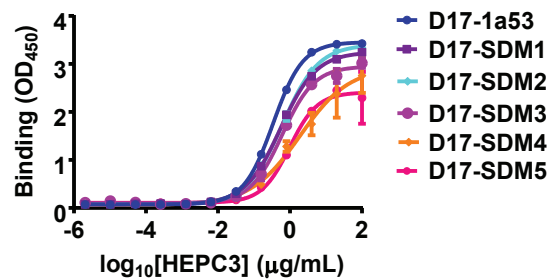


Figure S3. C110 cleared three genetically distinct genotype 1a infections, related to Figure 2. (A) Maximum likelihood phylogenetic tree of 5 kb hemigenomic nucleotide sequences obtained by single-genome amplification from plasma of C110 at longitudinal time points throughout the course of infection, with Bole1a and strain H77 as outgroups. Bootstrap values greater than 90 are shown. Genetically distinct infections are highlighted in different colors, with days post initial infection at the time of sampling indicated. (B) Pairwise genetic distances between 374 genotype 1a unrelated 5' nucleotide hemigenomes from GenBank, and between the indicated groups of C110 sequences.

A

	mutations introduced					
	434	444	465	498	533	610
D17-1a53	N	H	F	P	D	D
D17-SDM1	H
D17-SDM2	D	H
D17-SDM3	D	.	Y	.	.	H
D17-SDM4	D	.	Y	.	V	H
D17-SDM5	D	Y	Y	S	N	H



B

	mutations introduced					
	438	442	445	461	466	475
D0-A4	L	F	N	R	A	A
D0-SDM	I	I	H	L	D	T

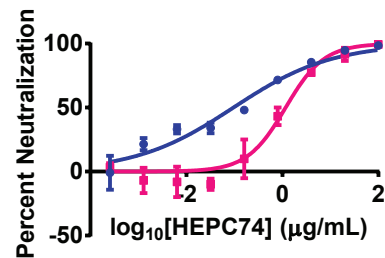
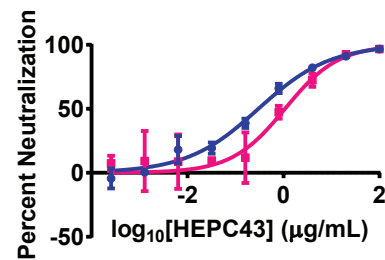
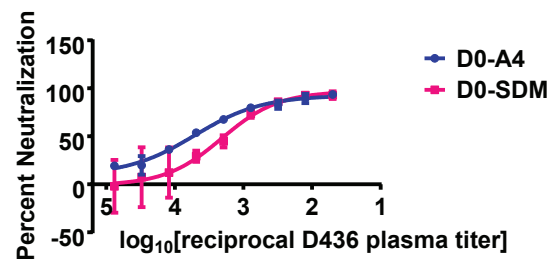


Figure S4. Site-directed mutagenesis identifies E2 substitutions responsible for partial resistance to HEPC3 binding or HEPC43 and HEPC74 neutralization, related to Figures 3-4. (A) Binding of serial dilutions of HEPC3 to E1E2 proteins in an ELISA. E1E2 strains tested include C117 D17-1a53 as well as this strain after introduction of the substitutions shown using site-directed mutagenesis (D17-SDM 1-5). One experiment representative of two independent experiments is shown. (B) Neutralization by C110 D436 plasma (**top**) HEPC43 (**middle**) or HEPC74 (**bottom**) of HCVpp expressing D0-A4 E1E2, or that strain after introduction of the substitutions shown (D0-SDM). One experiment representative of two independent experiments is shown.

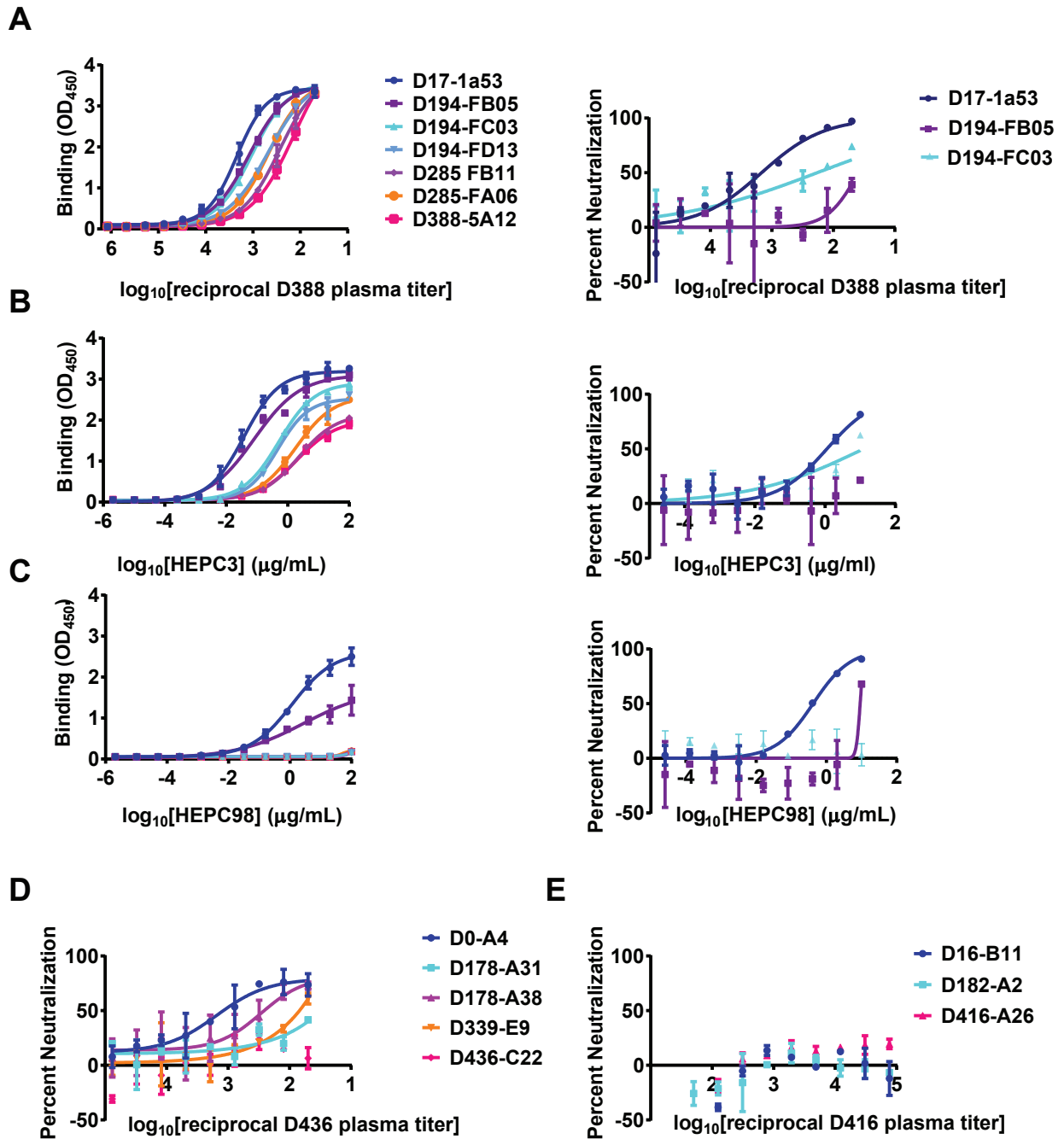


Figure S5. Second independent experiments: naturally selected substitutions in C117 or C110 E2 confer partial resistance to autologous plasma antibodies and autologous bNabs, related to Figure 3-4. (A-C) Binding to longitudinal C117 E1E2 proteins (left) or neutralization of longitudinal C117 HCVpp (right) by C117 D388 plasma IgG (A), HEPC3 (B) or HEPC98 (C). (D) Neutralization of longitudinal C110 HCVpp from Infxn 1 and 2 by C110 D436 plasma. (E) Neutralization of P29 HCVpp by P29 D416 plasma. All assays were performed in duplicate, and values are means +/- SD.

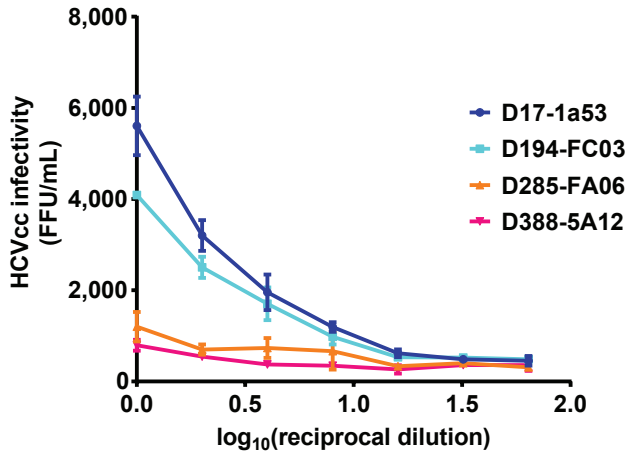
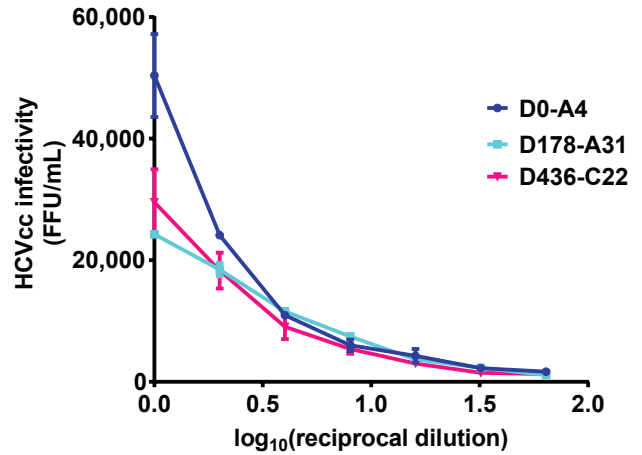
A**B**

Figure S6. Second independent experiment: infectivity of serial dilutions of chimeric replication competent cell culture virus (HCVcc) expressing longitudinal (A) C117 or (B) C110 E1E2 strains, measured as focus forming units/mL (FFU/mL) in Huh7.5.1 cells 48 hours after inoculation, related to Figure 5. Values are normalized for input HCV viral copy number. Assays were performed in duplicate, and values are means +/- SD.

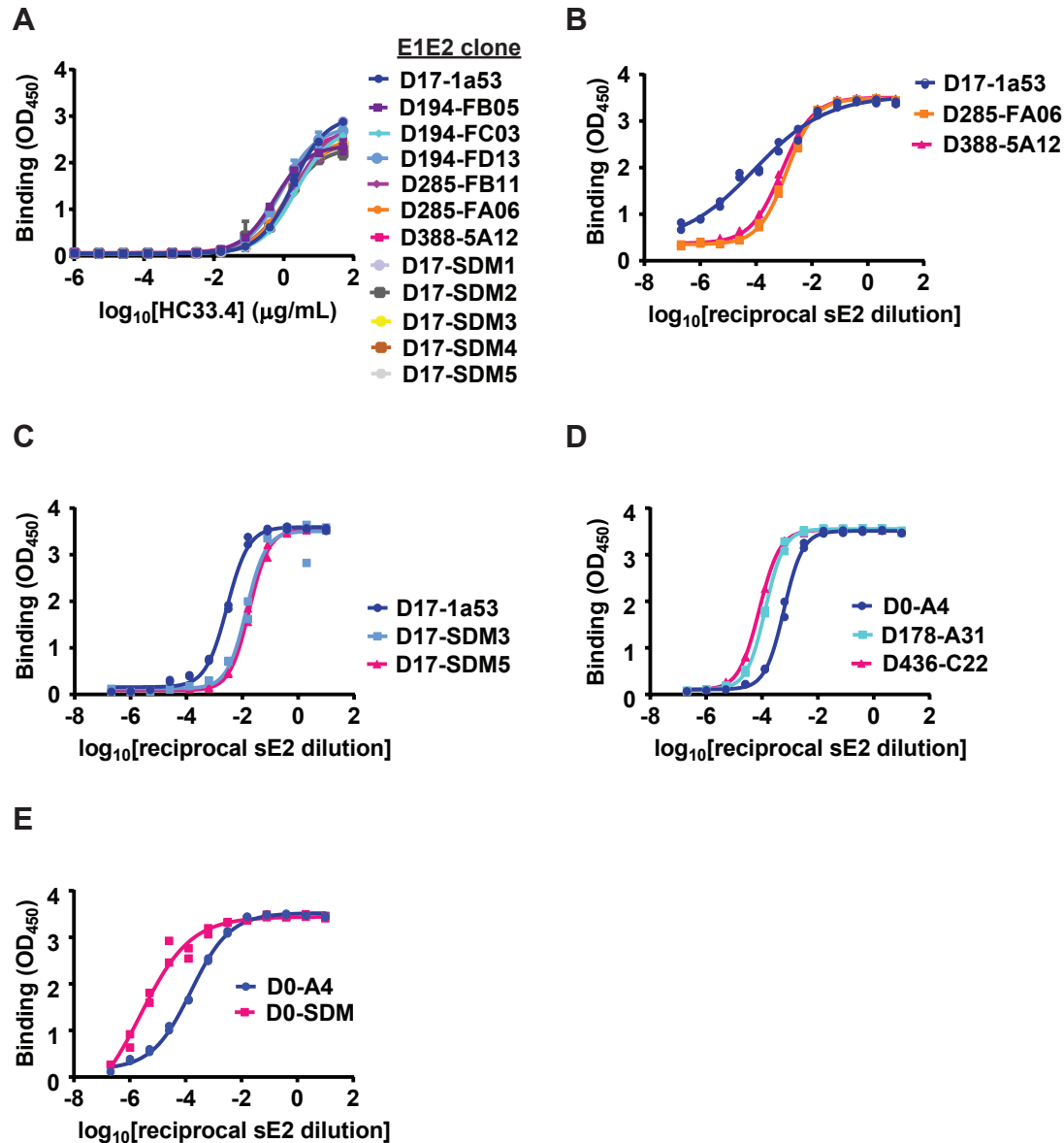


Figure S7. Relative quantitation of E1E2 and sE2 proteins, related to Figures 3 and 6. (A) Lysates of cells transfected with E1E2 expression plasmids were used to coat ELISA wells, then incubated with serial dilutions of control bNAb HC33.4. This bNAb binds to a linear, non-conformational epitope that is intact in all strains, so level of binding is proportional to the protein concentration. (B-E) Serial dilutions of sE2 supernatants were plated in ELISA wells and detected with anti-His antibody. Relative protein concentration in different supernatants were estimated from relative EC_{50} values of anti-His binding, and supernatants were adjusted to equivalent sE2 concentrations prior to CD81 and SR-B1 binding experiments. (B) C117 natural sE2 strains. (C) C117 SDM sE2 strains. (D) C110 natural sE2 strains. (E) C110 SDM sE2 strains.

Table S1. HCV substitutions arising over the course of C117, C110, and P29 infections. Changes away from (black text) or toward (blue text) the Bole1a sequence are indicated. *Only changes away from Bole1a are shown. Related to Fig 2.

Subject	Viral strains compared	Core-E1	E2			P7-NS5B
			HVR1	front layer	E2 (other)	
C117	D17-1a53 T/F#3 → D388-5A12		G390D	N434D	F465Y	H2030Q
			Q391R	H444Y	P498S	N2633S
			Y394R		D533N	R2720Q
			T395A		D610H	
			L402F			
		T404N				
C110	D0-A4 (Infxn1) → D178-A31 T/F#5 (Infxn 2)*	A217D	E384K	L438I	R461L	I753V
		V242I	H386Y	F442I	A466D	K781R
		D303G	V387T	N445H	A475T	T812A
		L345V	T388S		V570D	A828V
			G401S		I622V	R837N
			P405S		E641D	L876I
					D653N	I938L
						P978R
						K1250Q
						P1290S
						V1384A
						K1398R
						L1410M
						F1583L
				I1641V		
C110	D178-A31 T/F#5 → D436-C22 (Infxn 2 only)		K384G			F849L
			T387I			M936V
			A397S			V1408G
			F399L			
			A400V			
			F403L			
		S405P				
C110	D0-A4 (Infxn 1) → D1260-B3 (Infxn 3)*	A217D	E384G	N434K	D464K	I753V
		V242I	H386Y	N445H	A475T	K781R
		D303G	T388S		P498A	T812A
		L345M	S391A		K500Q	A828V
			A400V		E531V	R837S
			F403L		V570D	Y838H
			S404A		T577D	F849L
					S595A	M928I
					I622V	I938L
					E641D	T945A
						P978R
						I1044V
						P1290S
						V1384A
				L1410M		
				A1503T		
				F1583L		
				P1600L		
				I1641V		
C110	D1260-B3 → D1875-C3 (Infxn 3 only)		Y386H		T463V	K1250R
			G398R			
P29	D16-B11 T/F#1 → D416-A26				T463N	N958D
					Y527F	T985I

Residue (H77,1b09)	HEPC3 contact	HEPC74 contact	HEPC3 binding (H77)	HEPC74 binding (H77)	HEPC43 binding (H77)	CD81LEL binding (H77)	HEPC98 binding (H77)
L402							X
P,S405							X
K,S408							X
I414	X						
N417	X						
G418	X						
S419	X						
W420						X	
H421		X					
I422						X	
S,R424			X	X	X		
T425			X	X	X	X	
L427	X	X	X	X	X	X	
N428	X		X	X	X	X	
C429	X		X	X	X	X	
N430	X	X					
E,D431	X	X					
N,H434	X	X		X			
T435	X	X					
G436	X	X	X	X	X		
W,F437		X	X	X	X	X	
L438	X	X	X	X	X	X	
A439	X	X					
G,A440	X	X	X			X	
L441			X		X	X	
F442	X	X	X			X	
Y443	X	X				X	
H445		X					
K446	X	X					
F447	X	X					
D448	X	X					
R455				X			
A499			X	X	X		
C503			X	X	X	X	
V515				X	X		
G517			X				
T518			X	X	X	X	
T519				X	X		
D520			X	X	X	X	
G523				X	X		
Y527						X	
W529	X	X	X			X	
G530			X	X	X		
A,E531	X	X					
D535			X	X	X	X	
W616			X	X		X	
C620						X	
I626					X		
T647					X		

Table S2. E2-contact and/or critical binding residues of HEPC3, HEPC74, HEPC43, HEPC98, and CD81LEL.

Positions identified as contact residues displayed $> 10 \text{ \AA}^2$ of buried surface area in the bNAb-1b09_{ecto} complex crystal structure. Binding residues for bNAbs and CD81LEL were identified by alanine scanning as described in Methods. Red: Contact and/or binding residues shared by any bNAb and CD81LEL. Related to Fig 7.

Table S3. T cell interferon gamma responses to overlapping peptides spanning the entire HCV polyprotein. Related to Fig 2.

Subject	Days post-infection	HCV amino acid position	Viral protein	Sequence recognized (# aa)
C117	46	No detectable T cell responses		
	110	No detectable T cell responses		
	194	No detectable T cell responses		
	285	No detectable T cell responses		
C110	912	No detectable T cell responses		
	1009	No detectable T cell responses		
	1267	1169-1177	NS3	LLCPAGHAV (9)
	1267	1243-1258	NS3	AYAAQGYKVLVLNPSV (16)
	1267	1983-1998	NS5A	WICEVLSDFKTWLKAK (16)
	1267	1987-1995	NS5A	VLSDFKTWL (9)
	1267	2526-2539	NS5B	KDVRCHARKAVAHI (14)
	1267	2903-2918	NS5B	NRVAACLRLKLGVPPLR (16)
P29	58	1073-1081	NS3	CINGVCWTV (9)
	114	1073-1081	NS3	CINGVCWTV (9)
	135	512-527	E2	SPVVVGTTDRSGAPTY (16)
	135	1073-1081	NS3	CINGVCWTV (9)
	135	1395-1403	NS3	HSKKKCDEL (9)